Inorg. Chem. **2008**, *47*, 3610−3616

Inorganic Chemistry
Article

Similar K@$Au_{10}Sn_{10}$ Polyhedra in the Markedly Different Structures of KAu_4Sn_6 and KAu_3Sn_3. Syntheses and Characterization

Bin Li and John D. Corbett*

Ames Laboratory-DOE and Department of Chemistry, Iowa State University, Ames, Iowa 50011

Received October 9, 2007

These compounds were synthesized by high-temperature reactions of the elements in welded Ta tubes and characterized by X-ray diffraction methods and linear muffin-tin orbital (LMTO) calculations. AAu_4Sn_6 (A = K, Rb) have a new structural type (*Fddd*, $Z = 8$), and KAu_3Sn_3 (*Pmmn*, $Z = 2$) is isostructural with $SrAu_3In_3$. Both orthorhombic structures contain similar condensed K@$Au_{10}Sn_{10}$ polyhedral building blocks, which can be described as overall 6–8–6 arrangements of planar rings or, alternatively, as hexagonal prisms centered by K and augmented about the waists by 8-rings of Au and Sn. However, the 3D Au−Sn networks differ appreciably in both composition and the modes of condensation. In KAu_3Sn_3, the prisms stack by sharing both hexagonal faces with like neighbors along *a*, whereas those in KAu_4Sn_6 condense in a complex zigzag network. Compared with related indium systems, the structure change from KAu_4In_6 ($P\bar{6}m2$, $Z = 1$) to KAu_4Sn_6 apparently illustrates the effect of complex factors such as atom size and valence electron counts on structure, whereas the $SrAu_3In_3$ and KAu_3Sn_3 pair are isotypic. Both compounds are Pauli-paramagnetic and inert to water at room temperature for several days. Tight-binding electronic structure (LMTO) calculations emphasize the dominance and strength of the heteroatomic Au−Sn bonding.

Introduction

Exploratory synthesis in solid-state chemistry has led to the discovery of many new materials with novel structural and bonding features.[1] However, understanding the complex structures possible in solid-state chemistry is still very much in its youth as far as the prediction of what compounds and structures are possible, even in moderately sized regions of phase space. Thus exploratory synthesis remains an essential and active endeavor that is at the same time often exciting and challenging because of the numerous unprecedented, even unimaginable, compounds that can be found. Here, we report two more examples in terms of the syntheses and characterizations of two new compounds, KAu_4Sn_6 (**I**) and KAu_3Sn_3 (**II**), in which different atom proportions and valence electron counts afford a great deal of structural differentiation.

Recently, several new phases have been discovered in alkali-metal−Au−In systems, such as AAu_4In_2,[2] $A_{\sim 0.7}Au_2In_2$, AAu_4In_6, and $K_{1.76}Au_6In_4$ (A = K, Rb),[3] which all exhibit different tunnel-like structures. These as well as the novel inertness of some of these compounds to air and water at room temperature motivated us to explore other compounds and structures in similar systems. Moreover, tight-binding linear muffin-tin orbital (LMTO) electronic structural calculations on both AAu_4In_2 and AAu_4In_6[2,3] suggested that isostructural compounds with electron-richer main-group element substitutions might exist inasmuch as the major Au−In bonds still show substantial bonding character at the Fermi levels. This might also explain the existence of the evidently isotypic pair KAu_4In_2[2] and KAu_4Sn_2.[4] (The latter was characterized in a different acentric space group, but the two appear to be the same structure.) Moreover, comparison of many polar intermetallic compounds in alkali-

* Author to whom correspondence should be addressed. E-mail: jcorbett@iastate.edu.

(1) (a) Corbett, J. D. In *Chemistry, Structure and Bonding of Zintl Phases and Ions*; Kauzlarich S., Ed.; VCH Publishers: New York, 1996; Chapter 3 and other chapters. (b) Corbett, J. D. *Angew. Chem. Int. Ed.* **2000**, *39*, 670. (c) Belin, C. H. E.; Charbonnel, M. *Prog. Solid State Chem.* **1993**, *22*, 59.
(2) Li, B.; Corbett, J. D. *J. Am. Chem. Soc.* **2006**, *128*, 12392.
(3) Li, B.; Corbett, J. D. *Inorg. Chem.* **2007**, *46*, 6022.
(4) Sinnen, H.-D.; Schuster, H.-U. *Z. Naturforsch., B: Chem. Sci.* **1978**, *33*, 1077.
(5) (a) Liu, S.; Corbett, J. D. *Inorg. Chem.* **2004**, *43*, 4988. (b) Dai, J.-C.; Corbett, J. D. *Inorg. Chem.* **2006**, *45*, 2104. (c) Li, B.; Corbett, J. D. *Inorg. Chem.* **2006**, *45*, 8958. (d) Hoffmann, D.-R.; Pöttgen, R. *Z. Anorg. Allg. Chem.* **1999**, *625*, 994. (e) Dai, J.-C.; Corbett, J. D. *Inorg. Chem.* **2007**, *46*, 4592.

10.1021/ic701997x CCC: $40.75
Published on Web 03/18/2008

or alkaline-earth systems of indium versus tin[2,3,5] shows that tin is more diverse in the formation of nominal Zintl phases with either homoatomic or heteroatomic polyanions in binary or higher-order systems.[6,7] Inclusion of a third heteroelement also appears to be a very effective route to diverse new cluster structures beyond the binary systems, as has been demonstrated many times in alkali-metal−M−In systems (M = Li, Zn, Mg, Au).[2,3,8] As expected, the new phases in the alkali-metal−Au−Sn systems reported here contain similar building blocks: potassium-centered polyhedra, K@Au$_{10}$Sn$_{10}$, with a 6–8–6 ordering of planar rings of different sizes. A new structural type is observed for KAu$_4$Sn$_6$ (**I**, *Fddd*), quite different from that of KAu$_4$In$_6$ ($P\bar{6}m2$),[3] whereas KAu$_3$Sn$_3$ (**II**, *Pmmn*) is isostructural with SrAu$_3$In$_3$.[9]

Experimental Section

Syntheses. All materials were handled in N$_2$-filled gloveboxes with moisture levels below 1 ppm (vol). Both **I** and **II** were synthesized via high-temperature reactions of 99.995% gold, 99.98% tin (Ames Laboratory), and 99.95% potassium (Alfa-Aesar). The weighed elements were welded into tantalum tubes that were in turn sealed in evacuated fused-silica jackets by methods and techniques described previously.[10] Single crystals of **I** and **II** were first obtained from the compositions KAu$_4$Sn$_6$ and KAu$_2$Sn$_2$, respectively, that had been designed to gain the tin analogues of KAu$_4$In$_6$ and K$_{0.77(4)}$Au$_2$In$_2$,[3] respectively. However, neither of these targeted compounds formed. The product of the first reaction has the same composition as KAu$_4$In$_6$ but a different structure, whereas the second yields KAu$_3$Sn$_3$ instead. Pure phases (that is, >95% purity) were subsequently obtained from reactions of the appropriate compositions, as judged from comparisons of each Guinier powder pattern with that calculated from the refined structures and a conservative estimate of the detection limit of a second phase. The reaction samples were heated at 650 °C for 4 h, cooled at 5 °C/h to 350 °C, held there for 160 h to grow crystals, and cooled to room temperature at 5 °C/h. Both are silvery, brittle, and inert to air at room temperature. Both also appear to be kinetically inert to water at room temperature for at least 5 days, considering that their powder patterns afterward showed no changes in line intensity, breadth, or position. A Rb analogue of **I** is also stable according to its powder pattern, with orthorhombic unit cell dimensions of a = 8.759(2), b = 10.096(2), and c = 24.207(5) Å.

X-Ray Studies. Powder diffraction data were collected with the aid of a Huber 670 Guinier powder camera equipped with an area detector and Cu Kα radiation (λ = 1.540 598 Å). Powdered samples were homogeneously dispersed on a Mylar sheet with the aid of a little vacuum grease. Peak searches, indexing, and least-squares refinements for cell parameters were done with the WinXPOW program.[11] Single crystals were selected from the products in a glovebox and, as a standard precaution, sealed in capillaries. Single-crystal diffraction data for each were collected at 293 K over a 2θ range of ~3° to ~57° with the aid of Mo Kα radiation and a Bruker SMART APEX CCD diffractometer in the form of three sets of 606 frames, each with 0.3° scans in ω and exposures of 10 s per frame. The unit cell parameters were determined from diffractometer data for about 900 indexed reflections. The reflection intensities were integrated with the SAINT subprogram in the SMART software package[12] and were corrected for absorption numerically with the aid of the program X-shape in STOE software[13] after correction for Lorentz and polarization effects.

Table 1. Crystal and Refinement Data for KAu$_4$Sn$_6$ (**I**) and KAu$_3$Sn$_3$ (**II**)

compounds	KAu$_4$Sn$_6$	KAu$_3$Sn$_3$
fw	1539.11	986.07
space group, Z	*Fddd* (No. 70), 8	*Pmmn* (No. 59), 2
unit cell (Å), a	8.709(2)	4.6614(9)
b	10.028(2)	7.659(2)
c	24.157(5)	9.271(2)
V (Å^3)	2109.8(7)	331.0(1)
d_{calcd} (g/cm^3)	9.691	9.895
μ, mm^{-1} (Mo Kα)	69.66	77.88
data/restraints/param.	647/0/30	482/0/26
GOF on F^2	1.105	0.993
R1/wR2 [$I > 2\sigma(I)$]	0.041/0.101	0.041/0.089
R1/wR2 (all data)	0.047/0.104	0.043/0.090
largest diff. peak and hole (e Å^{-3})	4.61, −2.80	3.06, −2.58

Both structural solutions were obtained by direct methods and refined by full-matrix least-squares on F_o^2 using the Bruker SHELXTL 6.1 software package.[14] The $|E^2 - 1|$ values obtained for both from intensity statistics gave good indications of centrosymmetric space groups. Systematic absences in the data sets indicated that **I** is face-centered with the only possible space group *Fddd* (No. 70), whereas **II** is primitive with possible space groups of noncentric $P2_1mn$ (No. 31) or the centric *Pmmn* (No. 59). The latter turned out to be correct. Direct methods provided all five positions in each, of which two were assigned to Au, two to Sn, and one to the K atom according to peak heights and reasonable distances between them. The refinements, finally with anisotropic displacement parameters, converged at R1 = 0.041 and 0.041 and wR2 = 0.101 and 0.089 ($I > 2\sigma(I)$) for **I** and **II**, respectively. Residual peaks (<5 e Å^{-3}) and holes in final ΔF maps all lay near different heavy atoms.

Some crystallographic and refinement parameters for both compounds are given in Table 1; Table 2 contains the corresponding atom positional and isotropic displacement parameters, and Table 3 lists selected interatomic distances in both. More detailed crystallographic and refinement data and the anisotropic displacement parameters for the reported solutions are available in the Supporting Information (cif).

Physical Property Measurements. Magnetic susceptibility data for **I** (109.2 mg) and **II** (60.0 mg) were obtained from ground powders sealed under He in a container described elsewhere.[15] The magnetizations were measured over the range 2–350 K on a Quantum Design MPMS SQUID magnetometer. The data show almost temperature-independent paramagnetism at 30 kOe, ~1 × 10^{-4} and ~2 × 10^{-4} emu/mol for **I** and **II** compounds, respectively,

(6) (a) Ganguli, A. K.; Corbett, J. D.; Köckerling, M. *J. Am. Chem. Soc.* **1998**, *120*, 1223. (b) Sun, Z.-M.; Xia, S.-Q.; Huang, Y.-Z.; Wu, L.-M.; Mao, J.-G. *Inorg. Chem.* **2005**, *44*, 9242.
(7) (a) Bobev, S.; Sevov, S. C. *Inorg. Chem.* **2000**, *39*, 5930. (b) Bobev, S.; Sevov, S. C. *Angew. Chem. Int. Ed.* **2000**, *39*, 4108. (c) Bobev, S.; Sevov, S. C. *Inorg. Chem.* **2001**, *40*, 5361. (d) Bobev, S.; Sevov, S. C. *J. Alloys Compd.* **2002**, *338*, 87. (e) Bobev, S.; Sevov, S. C. *J. Am. Chem. Soc.* **2002**, *124*, 3359.
(8) (a) Li, B.; Corbett, J. D. *J. Am. Chem. Soc.* **2005**, *127*, 926. (b) Li, B.; Corbett, J. D. *Inorg. Chem.* **2006**, *45*, 8958. (c) Li, B.; Corbett, J. D. *Inorg. Chem.* **2005**, *44*, 6515. (d) Li, B.; Corbett, J. D. *Inorg. Chem.* **2006**, *45*, 3861.
(9) Muts, I. R.; Schappacher, F. M.; Hermes, W.; Zaremba, V. I.; Pöttgen, R. *J. Solid State Chem.* **2007**, *180*, 2202. Palasyuk, A.; Corbett, J. D. Unpublished.
(10) Dong, Z-C.; Corbett, J. D. *J. Am. Chem. Soc.* **1993**, *115*, 11299.
(11) *STOE WinXPOW 2.10*; STOE & Cie GmbH: Darmstadt, Germany, 2004.
(12) *SMART*; Bruker AXS, Inc.: Madison, WI, 1996.
(13) *XSHAPE 2.03*; Stoe & Cie GmbH: Darmstadt, Germany, 2003.
(14) *SHELXTL*; Bruker AXS, Inc.: Madison, WI, 2000.
(15) Guloy, A. M.; Corbett, J. D. *Inorg. Chem.* **1996**, *35*, 4669.

Table 2. Atomic Coordinates and Displacement Parameters ($Å^2 \times 10^3$) for KAu_4Sn_6 (**I**)[a] and KAu_3Sn_3 (**II**)

atom	Wyck.	*x*	*y*	*z*	*U*(eq)
Au1	16 g	1/8	1/8	0.3127(1)	14(1)
Au2	16 g	1/8	1/8	0.4316(1)	14(1)
Sn1	16 f	1/8	0.2695(1)	1/8	12(1)
Sn2	32 h	0.3753(1)	0.1225(1)	0.0096(1)	13(1)
K	8 b	1/8	1/8	5/8	19(1)
Au1	2 a	1/4	1/4	0.0710(1)	25(1)
Au2	4 e	1/4	0.5395(1)	0.5809(1)	26(1)
Sn1	2 a	1/4	1/4	0.3860(2)	23(1)
Sn2	4 e	1/4	0.5466(2)	0.8785(2)	23(1)
K	2 b	1/4	3/4	0.2598(7)	29(1)

[a] Second setting; origin at *i*.

Table 3. Selected Bond Lengths [Å] in KAu_4Sn_6 (**I**) and KAu_3Sn_3 (**II**) and Some of Their −ICOHP Values (eV/bond mol) from LMTO Calculations

KAu_4Sn_6			KAu_3Sn_3		
bond	distance	−ICOHP	bond	distance	−ICOHP
Au1−Sn2	2.792(1)	1.75	Au1−Sn2	2.8423(9)	1.72
Au1−Sn2	2.839(1)	1.66	Au1−Sn2	2.889(2)	1.69
Au1−Sn1	2.8508(6)	1.59	Au1−Sn1	2.921(2)	1.64
Au2−Sn1	2.7800(6)	1.75	Au2−Sn2	2.759(2)	2.13
Au2−Sn2	2.860(1)	1.45	Au2−Sn1	2.8504(7)	1.48
Au2−Sn2	2.877(1)	1.48	Au2−Sn1	2.860(2)	1.52
Au2−Au1	2.873(1)	1.20	Au2−Au2	2.837(1)	1.22
Sn1−Sn1	2.899(2)	2.30	Au2−Au2	3.224(2)	0.45
Sn1−Sn2	3.426(2)	0.40	Sn2−Sn2	3.116(3)	0.86
Sn2−Sn2	3.312(1)	0.56	Sn2−Sn2	3.320(2)	0.46
Sn2−Sn2	3.352(1)	0.43	K−Sn1	4.004(2)	
Sn2−Sn2	3.393(1)	0.29	K−Sn1	4.026(6)	
K−Sn1	3.565(1)		K−Sn2	3.498(3)	
K−Sn2	3.537(1)		K−Sn2	3.863(6)	
K−Sn2	4.090(1)		K−Au1	3.852(5)	
K−Au1	3.6460(5)		K−Au2	3.385(6)	
K−Au2	3.5909(5)		K−Au2	3.540(3)	

over 2–350 K after corrections for the container and the diamagnetic cores of the atoms. Graphical data for the magnetic susceptibilities are in the Supporting Information. The small changes in susceptibility with temperature for **I** may be caused by an impurity that could not be detected by X-ray powder diffraction.

Electronic Structure Calculations. In order to better understand the bonding in both structures, tight-binding electronic structure calculations were performed by means of the LMTO method in the atomic sphere approximation (ASA).[16] The radii of the Wigner−Seitz (WS) spheres were assigned automatically so that the overlapping potentials would be the best possible approximations to the full potentials, and no interstitial spheres were necessary with the default 16% overlap restriction.[17] The WS radii determined by this procedure were reasonable for all atoms: 1.52 Å for both Au; 1.62 Å for both Sn, 2.37 Å for K in **I**, 1.54 and 1.46 Å for Au1 and Au2, respectively, 1.66 and 1.56 Å for Sn1 and Sn2, respectively, and 2.25 Å for K in **II**.

Results and Discussion

Crystal Structures. The general overviews of KAu_4Sn_6 (**I**) and KAu_3Sn_3 (**II**) in Figures 1a and 2a illustrate the respective three-dimensional Au−Sn networks. Both are constructed from similar basic units, 20-vertex polyhedra centered by potassium, $K@Au_{10}Sn_{10}$, as shown in more local views of the general packing in Figures 1b and 2b, respectively. The individual polyhedra can be readily described as distorted hexagonal prisms that sandwich K together with eight additional Au/Sn atoms that are coplanar with K and lie about the prism waists in a distorted octagon, that is, an overall 6–8–6 arrangement of atoms in parallel rings oriented along *a*. However, the symmetry and arrangements of the two polyhedra are distinctly different. The polyhedra in **I** have 222 point symmetry, with four gold atoms in the each six-membered ring and two in the eight-membered ring, the rest being tin. The polyhedra in **II** have *mm*. symmetry, with alternating gold and tin in the six-membered rings and four of each in the eight-membered rings but with lower symmetry, the same as in the isotypic $SrAu_3In_3$.[9] The overall 6–8–6 plane populations are $Au_4Sn_2-Au_2Sn_6-Au_4Sn_2$ in **I** and $Au_3Sn_3-Au_4Sn_4-Au_3Sn_3$ in **II**. (In practice, the recognizable distortions of both polyhedral types means that only 18 of 20 atoms are plausibly bonded to the cation, as listed in Table 3. This limit omits pairs of 4.67 and 4.2 Å K −Au contacts about the waist of **I** and **II**, respectively.) The overall drive for the formation of these kinds of polyhedra can be interpreted as the need to give each cation, potassium here, as many close neighbors as possible from the more anionic Au−Sn network, given the variety of ways in which these ideal blocks are condensed, inasmuch as stoichiometry is a controlling variable. A common result is that the prismatic atoms about one center are simultaneously waist atoms in the neighboring units (Figure 1c), but the possible variations on this theme seem very large.

Many examples of polyhedral units with similar local structures have been reported, for example, 22-vertex $K@Mg_{12}In_{10}$ in $K_3Mg_{20}In_{14}$ (plus filler units)[18] and 21-vertex $A@Au_9In_{12}$ (A = K, Rb) and $Ae@Mg_5M_7In_9$ (Ae = Sr, Ba; M = Mg/In) in AAu_4In_6[3] and $AeMg_5In_3$,[19] respectively, both with 6–9–6 arrangements of planar rings. The network structure of the last is the inverse of that found in the isotypic $Ca_2In_4Au_3$ (with a change in cation site occupancy).[20] Similar alkaline-earth-metal-centered polyhedra, mainly based on pentagonal prisms instead, are observed in $BaAu_2Tl_7$,[21] $(Ba,Sr)Au_2In_2$,[5e] $BaTl_4$, and $(Sr,Ba)TIn_4$ (T = Ir, Pt).[22]

The principal difference between the present structures is the manner in which the ideal 20-vertex polyhedra are shared or condensed. The arrangement in **I** is complex according to its *Fddd* space group. The [100] section of KAu_4Sn_6 in Figure 1c shows how the eight-membered rings that lie about the prism waists of each share two trans Au−In edges with six-membered rings of neighboring polyhedra, and each six-membered ring (displaced by *a*/4) is shared laterally with two like rings and two eight-membered rings of neighboring polyhedra. (The bonds within layers in Figure 1c are differentiated by blue or red lines, and those between layers are represented by thinner black lines.) The polyhedra units

(16) Tank, R.; Jepsen, O.; Burkhardt, A.; Andersen, O. K. *TB-LMTO-ASA Program*, version 4.7; Max-Planck-Institut für Festkörperforschung: Stuttgart, Germany, 1995.
(17) Jepsen, O.; Andersen, O. K. *Z. Phys. B* **1995**, *97*, 35.
(18) Li, B.; Corbett, J. D. *Inorg. Chem.* **2006**, *45*, 3861.
(19) Li, B.; Corbett, J. D. *Inorg. Chem.* **2007**, *46*, 2237.
(20) Hoffmann, R.-D.; Pöttgen, R. *Z. Anorg. Allg. Chem.* **1999**, *625*, 994.
(21) Liu, S.; Corbett, J. D. *Inorg. Chem.* **2004**, *43*, 2471.
(22) Dai, J.-C.; Palasyuk, A.; Corbett, J. D. Unpublished research.

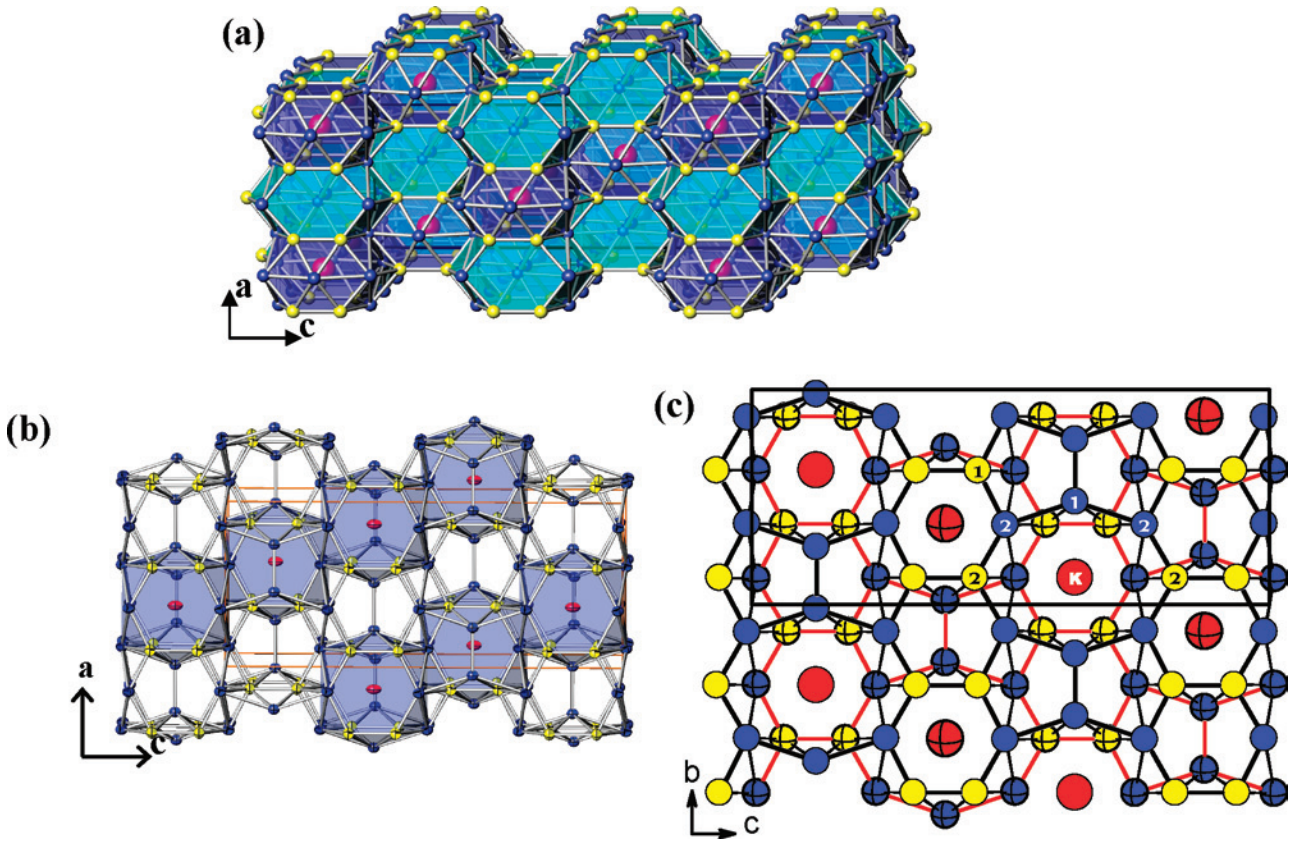

Figure 1. (a) General ~[010] section of KAu_4Sn_6 (**I**, *Fddd*) with a three-dimensional Au−Sn network composed of a single basic building unit. The Sn, Au, and K atoms are blue, yellow, and red, respectively. (b) A thin [010] section illustrating the stacking of potassium-centered 20-vertex polyhedron K@$Au_{10}Sn_{10}$ and empty spaces. The sequence changes with depth (see text). (c) A two-layer [100] section of the structure. The bonded atoms connected by thick black and red lines are at $y \sim +1/8$ (open spheres) and $y \sim -1/8$ (crossed), respectively, and the connections between layers are thinner black lines.

so described stack alternately along the vertical *a* axis (Figure 1b) with smaller K-free cavities generated by four neighboring centered polyhedra. The only interpolyhedral bond, Sn1−Sn1 = 2.899 Å, lies across this vacancy along *b*. The thin [010] section in Figure 1b also exhibits sloping parallel chains made of condensed polyhedra that are alternately displaced in depth by *a*/4. This is also perceptible in the more general view in Figure 1a. Moreover, displacement of the entire Figure 1b section along the view by only ±*a*/4 yields similar chains that are tilted in the opposite direction, such that thicker sections become complicated through the overlap of many additional cluster chains, as appropriate to the diagonal glides in the *Fddd* space group. Overall, each centered polyhedron shares faces and edges with eight other like neighbors, with empty sites adjoining its basal hexagonal faces. Necessarily, only a thin two-layer section is projected in Figure 1c as well, in which inclined chains of alternating basal and waist planes running roughly along *c* also alternate along *b* with mixed chains of cavities and hexagonal faces.

On the other hand, the cation-richer *Pmmn* structure of KAu_3Sn_3 (**II**) in Figure 2b is also more simply condensed. The 20-vertex polyhedra share hexagonal faces along *a* to generate simple tunnel-like features with well-trapped cations, Figure 2b. The *bc* plane, Figure 2c, also shows how each eight-membered ring defining the polyhedral waist shares edges with four six-membered basal faces and two like eight-membered rings of neighboring polyhedra. Each six-membered ring (displaced by *a*/2) is condensed with four eight-membered waists of neighboring polyhedra. Compared with the eight neighboring polyhedra around each polyhedron in **I**, there are 10 in **II**, including the two empty ones on basal faces along *a*. Such infinite tunnel-like structures have been observed in both AAu_4In_6 (A = K, Rb)[3] and $AeMg_5In_3$ (Ae = Sr, Ba),[19] in which columns of condensed 21-vertex polyhedra A@Au_9In_{12} and Ae@$Mg_5M_7In_9$ (M = Mg/In) stack along the shortest axes. Small 4-rings join these laterally.

Comparison of the present compounds with related indium phases is useful. For example, the similarly proportioned KAu_4In_6[3] is constructed in $P\bar{6}m2$ from 21-vertex K@Au_9In_{12} units, whereas these proportions in KAu_4Sn_6 generate a much more complex arrangement of 20-vertex polyhedra K@$Au_{10}Sn_{10}$, Figure 1. The change can be at least partly attributed to the six-electron difference in valence electrons per formula unit. Earlier electronic calculations on KAu_4In_6 indicated that more than four additional electrons would begin to fill major Au−In antibonding states, but of course this relationship says nothing about the dependence of stability on electron count or on any alternate structures. On the other hand, compound **II**, KAu_3Sn_3, is isostructural with the recently discovered $SrAu_3In_3$,[9] which is also the only other known example of this structure type. There is only a two-electron difference between these, thanks to a lower electron count for the p element in the latter and the one

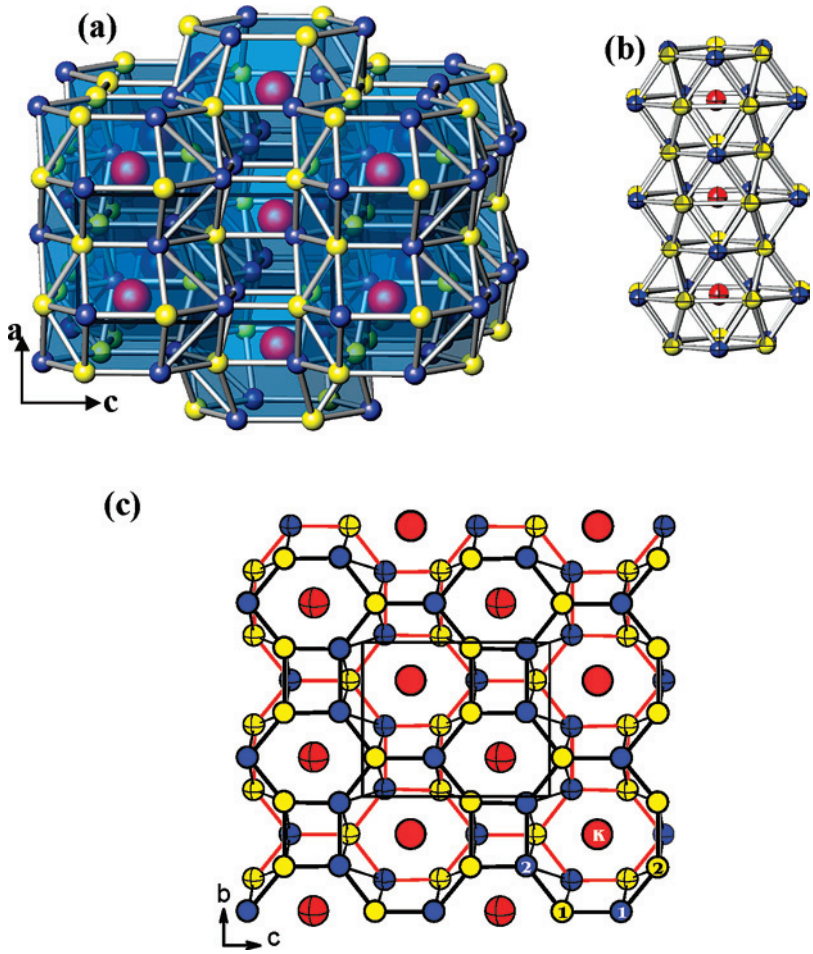

Figure 2. (a) General ~[010] view of KAu_3Sn_3 (**II**, *Pmmn*) with a three-dimensional Au−Sn network composed of a single basic building unit. The Sn, Au, and K atoms are blue, yellow, and red, respectively. (b) The K-centered 20-vertex polyhedra $K@Au_{10}Sn_{10}$ stacking directly along the *a* axis. (c) A two-layer [100] section of the structure. The bonded atoms connected by thick black and red lines are at $y \sim 1/4$ (empty) and $y \sim 3/4$ (crossed), respectively, and the bonding connections between layers are thinner black lines.

additional electron provided by Sr. There is also only a two-electron difference between the isotypic KAu_4In_2[2] and KAu_4Sn_2.[4] An attempt to synthesize the KAu_3In_3 analogue of KAu_3Sn_3 failed, presumably because of the relatively more stable $K_{0.77(4)}Au_2In_2$.[3] Of course, the similar sizes of K and Sr and of Sn and In are also important in these pairs of isotypic structures.

The Au−Sn bond distances in both **I** and **II** have similar and rather narrow ranges, 2.79–2.88 Å (KAu_4Sn_6) and 2.76–2.92 Å (KAu_3Sn_3). These lengths are comparable to those in KAu_4Sn_2[4] (2.74–2.99 Å) and in K_3AuSn_4 (~2.78 Å).[23] There is only a single Au−Au contact in **I**, Au1−Au2 (2.87 Å) within the six-membered ring, which is somewhat long compared with the Pauling single-bond metallic diameter of 2.68 Å.[24] However, this is not a sufficient determinant as there are a variety of size, bonding, and packing factors that go into a distance determination in these highly condensed results. There are several kinds of Sn−Sn contacts in **I**, the noteworthy small *d*(Sn1−Sn1) (2.90 Å) between two polyhedra noted above, Sn2−Sn2 (3.31 and 3.35 Å) between six- and eight-member rings, and a long Sn2−Sn1 (3.43 Å) within the eight-membered ring. The last three are distinctly greater than those in K_3AuSn_4 (2.91–3.12 Å),[22] but they still represent bonding interactions according to the electronic structure calculations that follow. In **II**, there are two independent Au−Au interactions, Au2−Au2 (3.22 Å) within the eight-membered ring and Au2−Au2 (2.84 Å) between six- and eight-membered rings. Conversely, the greater Sn2−Sn2 (3.32 Å) bond occurs between rings, and the shorter Sn2−Sn2 (3.12 Å) within the eight-member ring. All of the interactions noted represent non-negligible integrated crystal orbital Hamilton population (−ICOHP) values (below), and they are marked as bonds in both figures. Certainly the ranges cited must reflect the obvious complexities of the extensive condensation of augmented hexagonal prisms necessary to yield different overall compositions and the accompanying electronic factors.

Electronic Structure and Chemical Bonding. The densities-of-states (DOS) for KAu_4Sn_6 (**I**) and KAu_3Sn_3 (**II**), Figure 3a and c, respectively, show broad bands with finite densities around E_F, indicating metallic characteristics, and both appear to be Pauli-paramagnetic (Supporting Information). The large DOS peaks around −5 eV in both structures originate mainly from the Au 5d orbitals. The

(23) Zachwieja, U.; Müller, J.; Wlodarski, J. *Z. Anorg. Allg. Chem.* **1998**, *624*, 853.
(24) Pauling, L. *Nature of the Chemical Bond*, 3rd ed.; Cornell University Press: Ithaca, NY, 1960; p 403.

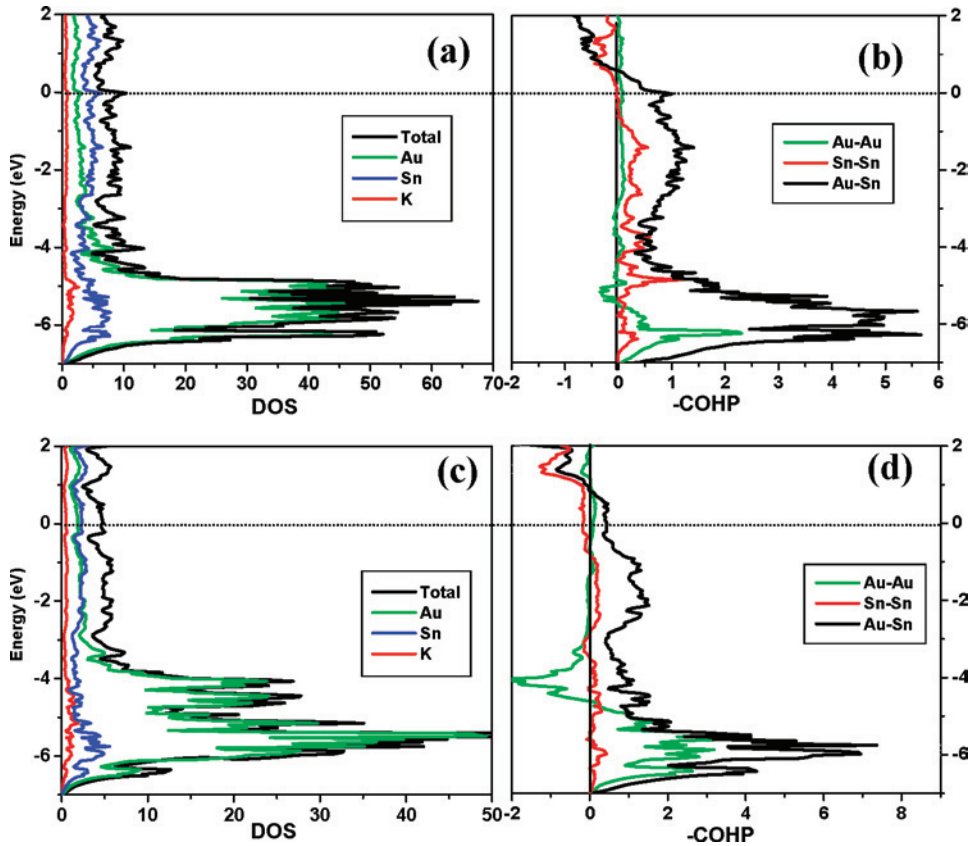

Figure 3. TB-LMTO-ASA electronic structure results for KAu_4Sn_6 (top) and KAu_3Sn_3 (bottom). (a, c) Total DOS (black) and partial DOS curves for Au (green), Sn (blue), and K (red). (b, d) −COHP curves for Au−Au (green), Sn−Sn (red), and Au−Sn (black) interactions in each structure. The dotted lines denote the corresponding Fermi levels. Note the different abscissa scales for the two compounds.

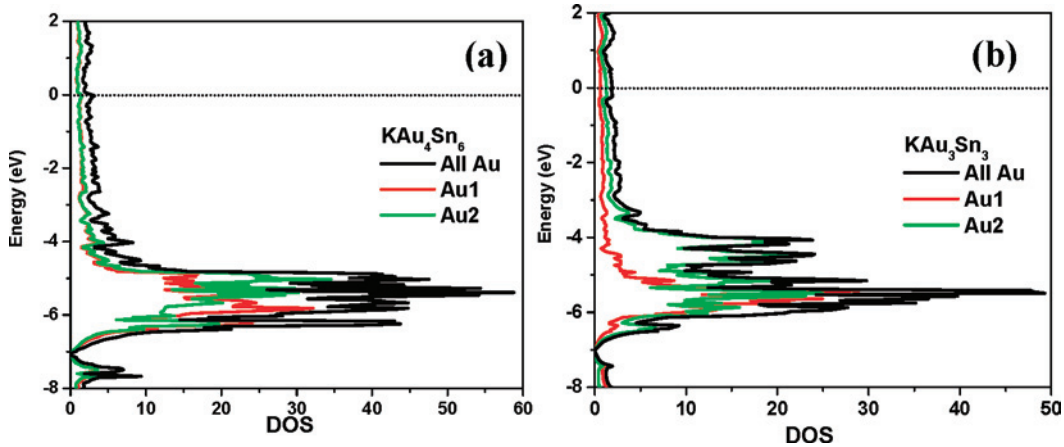

Figure 4. Partial DOS curves for Au in (a) KAu_4Sn_6 and (b) KAu_3Sn_3 calculated by TB-LMTO-ASA methods: all Au (black), Au1 (red), and Au2 (green). The dotted lines denote the Fermi levels. Large and different contributions from Au1 and Au2 are seen in KAu_3Sn_3.

two types of independent gold atoms in each are fairly well separated according to their partial DOS data plotted in Figure 4a,b. Those for **I** (4a) show the Au1 and Au2 bonding centers around −6 eV and −5 eV, respectively. A distinctly broader PDOS for Au in **II** (4b) that extends to −3.5 eV is spanned by contributions from 2.837 and 3.224 Å Au2−Au2 contacts (green curve). The antibonding contributions at the higher energy (Figure 3d) mainly come from the longer Au2−Au2 separation (Supporting Information). The Au1 sites in both structures display the smaller scalar relativistic changes. Note the relatively small (and characteristic) contributions of K to the DOS in both structures, Figure 3a and c. Similar characteristics also appear in both KAu_4In_6 and $K_{1.76(6)}Au_6In_4$.[3]

The crystal orbital Hamilton population (−COHP) analyses shown in Figure 3b and d for **I** and **II**, respectively, give good assessments of the relative contributions of the Au−Au, Au−Sn, and Sn−Sn bonding (overlaps). Particularly strong bonding is found for Au−Sn bonds in the former KAu_4Sn_6, but it must be noted that the relative numbers of independent Au−Au, Au−Sn, and Sn−Sn bonds in this structure vary as 1:12:7. The relatively small effects of the Au−Au bonds are thus understandable. More electrons would populate Sn−Sn antibonding states and lead to lessened stability. In

the latter KAu_3Sn_3, both Au−Sn and Au−Au interactions remain bonding at E_F, whereas the Sn−Sn bond shows a small antibonding behavior near there. The relative numbers of Au−Au, Au−Sn, and Sn−Sn bonds here vary as 1:4:1, so the heteroatomic bonding is less dominant but still major. Many structures of this type feature alternating atom types in their networks. The number of valence electrons (88.6 including Au d^{10}) corresponding to the energy at which Sn−Sn bonding is optimized is very close to the number present in the isostructural $SrAu_3In_3$ (88).[9]

The −ICOHP values were also determined for all network bonds among the Au and Sn atoms, Table 3. All values are reasonable relative to the bond distances, although of course the interrelationships are not linear; −ICOHP data are much more fundamental relatives to bond strengths. The Au−Sn values are quite large in both compounds, more than 1.4 eV/bond, suggesting they are dominant in energy as well as frequency and major factors in the structures formed. This characteristic as well as the observed atom distributions must originate in good part from the relatively large differences in the (Mulliken) electronegativities of these two atoms. Even though both Au1−Au2 and Au2−Au2 distances are somewhat long (2.873 Å in **I**, 2.837 Å in **II**), their −ICOHP values are quite large, about 1.2 eV/bond. It is worth noting that the very long 3.224 Å Au2−Au2 separation within the eight-member ring in **II** still has a non-negligible −ICOHP value, 0.45 eV/bond. Among all Sn−Sn bonds in **I**, only the short *d*(Sn1−Sn1) (2.899 Å) has a correspondingly large −ICOHP value, 2.30 eV/bond, whereas other Sn−Sn distances are all quite long and exhibit small but not negligible −ICOHP values.

Conclusion

Compared with the extensive prior studies of binary alkali-metal−tin systems, related ternary systems have been rarely explored. For example, only two unrelated compounds, KAu_4Sn_2[4] and K_3AuSn_4,[23] have been reported in the ternary potassium−gold−tin system. The existence of **I** and **II** further demonstrates that the addition of at least the particular heteroelement Au to the binary A−Sn systems is a very effective route to diverse new cluster structures. Both display similar basic building blocks, a potassium-centered 20-vertex $K@Au_{10}Sn_{10}$, but different proportions and three-dimensional Au−Sn networks. The two cases of different structures obtained for KAu_4Sn_6 (**I**) versus KAu_4In_6[3] and of the isostructural KAu_3Sn_3 (**II**) and $SrAu_3In_3$[9] indicate that more complex factors, such as atom sizes and valence electron counts, play roles in the new compounds. Thus, it is a general challenge to predict possible structures in even similar systems.

From another viewpoint, four relatively simple binary Au−Sn intermetallic compounds are known in this region, Au_5Sn and $AuSn_x$ for $x = 1$, 2, and 4.[25] Reduction of these by active metals also leads to the very different and evidently rich field of ternary polyanionic Au−Sn phases and much new chemistry. Reports on two more compounds in the ternary potassium−gold−tin system with novel structures are in preparation.

Acknowledgment. We are indebted to S. Budko for the magnetic susceptibility data. This research was supported by the Office of the Basic Energy Sciences, Materials Sciences Division, U.S. Department of Energy (DOE) and was performed in the Ames Laboratory, which is operated for DOE by Iowa State University under Contract No. DE-AC02-07Ch11358.

Supporting Information Available: Refinement parameters for KAu_4Sn_6 (**I**) and KAu_3Sn_3 (**II**) in cif format, figures of magnetic susceptibility data for both phases, and −COHP data for Au−Au bonds in **II**. This material is available free of charge via the Internet at http://pubs.acs.org.

IC701997X

(25) Villars, P.; Calvert, L. D. *Person's Handbook of Crystallographic Data for Intermetallic Phases*, 2nd ed.; American Society of Metals: Metals Park, OH, 1991, p. 433.